



Megathrust-driven crustal deformation revealed by fore-arc seismicity changes over subduction earthquake cycles

Felipe Aron^{*1,2,3}, Mauricio Bucca⁴, Dietrich Lange⁵

(1) Department of Earth and Atmospheric Sciences, Cornell University, Ithaca, New York 14853, USA

(2) Department of Geological Sciences, Stanford University, Stanford, California 94305, USA

(3) Departamento de Ingeniería Estructural y Geotécnica, Pontificia Universidad Católica de Chile, Vicuña Mackenna 4860, Macul, Santiago, Chile

(4) Department of Sociology, Cornell University, Ithaca, New York 14853, USA

(5) GEOMAR Helmholtz Centre for Ocean Research Kiel, Wischhofstr. 1-3, 24148, Kiel, Germany

*Contact email: felipearon@stanford.edu

Abstract. How important is the occurrence of great subduction earthquakes in driving permanent, long-term crustal deformation over convergent plate boundaries? We use the global catalogs of earthquakes and moment tensors to examine the style and character of upper-plate seismicity associated with great subduction events worldwide ($\geq M_w 7.7$) since 1976. The intraplate events are located inside the forearc wedge above the rupture areas; our search spans the full time series of the catalog, capturing the seismic behavior of the upper plate over the different stages of the subduction seismic cycle. Within the detection limits of the catalog, between 61% and 83% of the cases were upper plate earthquakes exhibit periods of increase seismicity rate and magnitude above background levels were induced by megathrust ruptures. That correlation is stronger for normal fault events than reverse or strike-slip earthquakes. For any given subduction zone, the summation of the seismic moment (M_o) accounted by the forearc normal fault aftershocks appears to have a positive correlation with the M_o of the subduction earthquake—the larger the megathrust events the larger the energy released by forearc aftershocks. Our results suggest that great subduction events may be important contributors of stress to produce permanent extension in the forearc.

Keywords: Subduction earthquakes, triggering of crustal earthquakes, forearc permanent deformation

1 Introduction

Following the 2010 Maule and 2011 Tohoku earthquakes, the upper plate overlying the rupture areas experienced a significant change in their seismic behavior. Both the rate of seismicity and total moment released by the forearc, intraplate events exceeded by far what had been observed in these regions preceding the main shocks (e.g., Hasegawa et al., 2012; Lange et al., 2012). But how likely are large, upper plate aftershocks after a great megathrust event?

In a recent study, Gomberg and Sherrod (2014) found evidence that, over a 1-year time window, the rate of

seismicity in the overriding plate and in some examples, the magnitude reached by upper plate earthquakes, increased with respect to background activity after great subduction ruptures ($M > 8.6$).

It has been suggested that in the Maule earthquake region and perhaps elsewhere, subduction earthquakes may be important in reactivating faults in the upper plate, producing permanent deformation of the forearc and shaping its structural grain (e.g., Aron et al., 2013, 2015; Dielforder et al., 2015). If that hypothesis holds true, one would expect to see a significant stress perturbation in the seismic behavior of the upper plate following megathrust earthquakes. Here we use the Global CMT (gCMT) catalog (Ekström et al., 2012) to examine the style and character of upper plate earthquakes associated with great subduction events. We test the hypothesis using standard techniques in statistical seismology to answer the following questions: After a great megathrust earthquake, (1) is there an increase in upper plate seismicity following large events?, (2) is there an increase in the moment released by upper plate events?, and (3), is there a change in the kinematic style of the upper plate events?

We show evidence that most of the great subduction events triggered upper plate seismicity in the near-field overlying the rupture, predominantly normal faulting but in some cases thrust and strike-slip as well. We show how the magnitude of these triggered events scales proportionally to the size of the megathrust. Finally, we discuss the implications of our findings for the long-term structural configuration of the forearc and for seismic hazard assessments.

2 Methods and Results

2.1 Subduction earthquakes and near-field volume

We have searched the entire Global CMT catalog between January 1, 1976 and January 31, 2015 for

subduction zones that have experienced large to great subduction earthquakes, with moment magnitudes equal or greater than 7.7 (Fig. 1). With almost 40 years of data, we have good coverage of coseismic and post-seismic phases of the great subduction events but we have a narrow window of observation for the interseismic period.

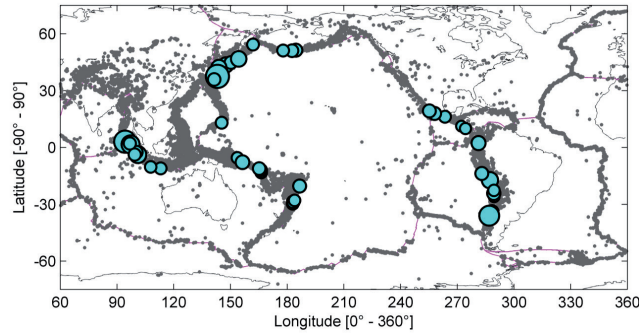


Figure 1. World map showing in light blue the epicenters of 44 subduction earthquakes $\geq M_w 7.7$ (gCMT catalog between January 1, 1976 and May 31, 2013). In gray are shown all the earthquakes recorded by the gCMT catalog.

We use a window-oriented approach to define near-field volumes based on a factor (β) of the megathrust rupture length (L ; based on empirical scaling laws). In map view, the extent of the near-field area is given by the distance along strike: $D = \beta L$, centered on the centroid epicenter, and the distance from the trench to the volcanic arc, perpendicular to the margin, so the segment encloses the entire forearc-arc region of the plate boundary over the subduction rupture. These criteria to determining near-field areas resulted in 18 segments (see Fig. 2 below), covering approximately 45% of the world forearc regions.

2.2 Upper plate vs. megathrust seismicity and kinematics

The Slab1.0 surface (Hayes et al., 2012) is used to separate earthquakes nucleated on the plate interface from events nucleated in the upper plate wedge, considering a safe range of depth-tolerance of ± 10 km above and below the slab, which represents the 3-D volume of the slab or megathrust. Using the principal axes of the earthquakes (P, T and B) we classify the events according to their kinematics (normal, reverse, strike-slip, and “odd”) following the scheme proposed by Frohlich (1992). We consider subduction events as reverse fault earthquakes close to the Slab1.0 model (vertical distance < 10 km), with one of the nodal planes oriented similarly to the slab surface—all the rest are intraplate (upper or lower) events.

2.3 Time series analysis

We analyze how the occurrence of the 44 identified strong megathrust earthquakes correlates over time, at each of the 18 near-field segments, with the following

variables: (a) increments in number of upper plate seismic events, (b) increments in moment release rate by those events and (c), kinematic style of the triggered events. In each segment, time is discretized in bins of equal width—ranging between 100 and 1,000 days—and same center points for both series: upper plate and subduction events. At each time bin, we count the number of events and calculate the total moment and moment magnitude of the bin. To further investigate the correlation of the cycles of moment release by subduction events with changes in seismicity rate and moment release rate in the upper plate, we produce a binary analysis of the full time series, searching for peaks relative to background activity. We define the peaks over the series in terms of both M_o (and M_w) total and number of events per time (N_r/t), as values that exceed a background threshold estimated from 99% confidence intervals (CI) for these variables, using nonparametric bootstrap resampling with replacement methods. Finally, we redefine the series in terms of zeroes and ones. We assign the value of 1 or true to bins exceed the defined background threshold (peak) or 0 otherwise (no-peak).

2.4 Megathrust earthquakes vs. upper plate peaks of seismicity

First we test at each of the defined segments how well peaks of increasing seismicity and moment release rates correlate in the upper plate to peaks in seismic activity of subduction earthquakes. We determine a correlation coefficient as the percentage of all the upper plate peaks that coincide in time with peaks of megathrust moment release using the following expressions:

$$\rho_{Mw} = \frac{\sum_{i=1}^{\#bins} \mathbf{1} \{UP_{Mw\ peak}(i) = 1 \mid MT_{Mw\ peak}(i) = 1\}}{\sum_{i=1}^{\#bins} \mathbf{1} \{UP_{Mw\ peak}(i) = 1\}} \quad (1)$$

$$\rho_{Nr} = \frac{\sum_{i=1}^{\#bins} \mathbf{1} \{UP_{Nr\ peak}(i) = 1 \mid MT_{Mw\ peak}(i) = 1\}}{\sum_{i=1}^{\#bins} \mathbf{1} \{UP_{Nr\ peak}(i) = 1\}} \quad (2)$$

where UP, MT, refer to upper plate and megathrust series, and Mw and Nr denotes peaks of the variables Mw total, or Nr/t respectively. The index ρ goes from 0 to 1 and can be read as the percentage of upper plate peaks that occurred in the same time range (bin position) than a peak of subduction earthquakes. A value of zero means that all the upper plate peaks do not coincide in time with peaks of subduction events, i.e., they occurred during the interseismic period, or that there were no peaks in the upper plate at all, whereas $\rho = 1$ indicates a perfect correlation. The results of maximum ρ_{Mw} and ρ_{Nr} calculated on each of the 18 segments are shown in Figure 2 and Table 1. Over the majority of the segments, the occurrence of peaks in the upper plate series is strongly correlated with the occurrence of peaks of subduction earthquakes, as shown by the high values of ρ .

2.5 Moment magnitude correlation

Our final test to correlate the behavior of upper plate seismicity to occurrence of great subduction earthquakes is to investigate possible scaling relations of moment release between megathrust events and triggered upper plate earthquakes. We select at each segment the bins in the subduction earthquakes time series with M_w total > 7.6 and compare them to the values of M_w release of the corresponding upper plate time bins, independently for each kinematic type. Using a least squares fit linear model, an increase of total moment magnitude by megathrust earthquakes accounts for a maximum of 47.8% of the variation in the total moment magnitude increase of upper plate normal fault events, over an aftershock time window of 1,000 days. That correlation is much weaker for reverse and strike-slip kinematics, reaching maximum percentage values of R^2 of 8.1% and 6.8% respectively.

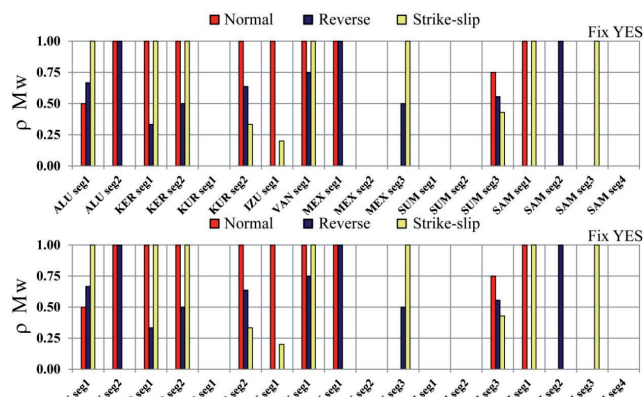


Figure 2. Peak correlation analysis of ρ_{Mw} (upper panel) and ρ_{Nr} (lower panel) for the 18 studied subduction segments, separated by fault kinematics. Values for each segment are calculated using equations (1) and (2).

Table 1: Percentage of total analyzed segments with $\rho \geq 0.5$ and $\rho = 1$

Kinematics	% $\rho_{Mw} \geq 0.5$	% $\rho_{Mw} = 1$	% $\rho_{Nr} \geq 0.5$	% $\rho_{Nr} = 1$
All*	72.2	66.7	77.8	77.8
Normal	55.6	44.4	66.7	61.1
Reverse	50.0	16.7	55.6	22.2
Strike-slip	38.9	38.9	50.0	38.9

*At least one of the kinematic style shows a peak correlation

3 Discussion

3.1 Triggering of upper plate earthquakes

The results from the binary analysis of the time series show that between 77% and 83% of the cases, great subduction events are responsible of peaks of Nr/t above background in the upper plate for at least one kinematic style. In 61-78% of the cases, upper plate peaks occurred only contemporaneous to a peak in subduction activity (Table 1). In terms of the magnitude reached by upper

plate events, our analysis shows a strong correlation as well. The percentage of the cases in which peaks above background in the upper plate are accompanied by peaks of subduction earthquakes range between 61% and 72%. For the majority of the studied subduction zones, periods of significant seismicity in the forearc are more likely to follow great subduction earthquakes than occur interseismically. But perhaps more importantly, we have found that this relation is stronger in the case of normal fault events. As discussed in the following section, this finding may have implications for the mechanisms and style of permanent deformation of the forearc, and for seismic hazard as well.

3.2 Kinematics of subduction-triggered events and implications for seismic hazard

Our analyses suggest that periods of high intraplate seismicity on forearc normal faults correlate better to an increase in subduction activity compared to reverse and strike-slip kinematics. The most outstanding examples are the upper plate events triggered by the great 2010 Maule and 2011 Tohoku earthquakes. Estimations of Coulomb stress change on the reactivated crustal faults in Chile and Japan show high stresses for normal faulting, indicating that these structures were properly oriented to slip under the loading conditions imposed by the megathrust earthquakes. In general, the shallowly plunging extensional axes of the crustal normal fault aftershocks tend to be oriented at high angle respect to the trench axis, indicating a component of stretching parallel to the heave of the megathrust. Studies using stress inversions from moment tensors of the world catalog and local networks show coseismic rotations of the principal axes of stress in the upper plate volume overlying the 2004 M_w 9.2 Sumatra-Andaman, 2010 M_w 8.8 Maule and 2011 M_w 9.0 Tohoku ruptures (e.g., Hardebeck, 2012). The maximum compressive stress axis was shallowly plunging before the earthquakes, approximately oriented parallel to the convergence vector, but following the main shock both the maximum and minimum principal stresses rotate so that the least principal stress axis becomes more horizontal, trending sub-perpendicular to the trench, while the compressive axis plunges at a higher angle. That switch in the state of stress occurs because the continent is mostly stretched in the direction of the coseismic rebound or heave of the megathrust, facilitating the reactivation of extensional features including surface tension cracks and shallow, intraplate normal faults (Baker et al., 2013). Those reactivations tend to occur in pre-existing structures that strike at a high angle to the maximum coseismic stretching orientation.

For the case of strike-slip and reverse faults, the correlation with subduction earthquakes is weaker over the time span of the catalog. In fact, they are more likely to occur interseismically. Nonetheless, we identified

several cases where significant triggering of these upper plate structures occurred. In many cases, large M 7 reverse and strike-slip events are observed across the entire magnitude range of analyzed megathrusts, contrary to the normal fault aftershocks which tend to reach maximum magnitudes following the megathrusts. This finding emphasizes the importance of the pre-existing structure, the ambient regional and local stresses, orientation of faults, and the location of the structures in space respect to the megathrust slip distribution.

Reverse faults triggered by subduction earthquakes tend to occur in the upper plate at the toe of the forearc wedge, up dip from the maximum coseismic slip zone (Li et al., 2014). This portion of the upper plate is more likely to experience shortening parallel to the heave of the megathrust, highly oblique to the trench. Several cases of thrust splay fault reactivations are clear, particularly in the Aleutians region, as previously observed after the great 1964 Alaska earthquake (Plafker, 1967), and in the outer forearc of the Sumatra subduction zone following the 2004-2005 Andaman and Nias great earthquakes (Sibuet et al., 2007).

Though there are many variables—many of them not addressed here—that control the dynamics of upper plate earthquakes, if there is a strong control in the seismic behavior of the forearc by the occurrence of great subduction earthquakes, we suggest that this would more likely apply to extensional faults. Our analysis of the magnitude scaling relation suggests that, compared to reverse and strike-slip events, forearc normal fault aftershocks satisfy better a linear relation between the size of megathrust events and that of the upper plate. For any given peak of subduction earthquakes, the total Mw accounted by triggered upper plate normal events over the coseismic/post-seismic period, calculated from the summation of Mo inside the bin, has a positive correlation with the total Mw of the subduction earthquakes—the larger the megathrust the larger the energy released by forearc normal fault aftershocks.

Given the relatively large magnitude and shallow depth of these triggered earthquakes, understanding their behavior in the context of the subduction seismic cycle becomes important for seismic hazards evaluation. In general, the Mw 7.0 crustal events both in Chile and Japan struck in sparsely populated areas with relatively good compliance of building codes and basic infrastructure; though a triggered normal fault with surface rupture did occur just 60 km south from the Fukushima nuclear plant. However, as population increases with concomitant land use and development, large crustal aftershocks pose a significant hazard to critical infrastructure. Most of the triggering cases bear common characteristics: they occur on preexisting structures that were favorably oriented to the stress field imposed by the subduction earthquake. This documented correlation between size of the main shock and that of the intraplate normal aftershocks, along with field studies of

these faults, suggest that the forearc structures should be as well incorporated in seismic hazard assessments in subduction zone regions.

Acknowledgements

We are grateful to many colleagues for enhancing our understanding of these processes, including Rick Allmendinger, José Cembrano, Matt Pritchard, Gabriel González, Muawia Barazangi, Tony Ingraffea, George Hilley, Erik Jensen, and Katie Keranen. Aron acknowledges support from CONICYT Beca Chile, NSF grants EAR-1118678 and EAR-1055981, and FONDECYT-3150116 Postdoctoral Grant, Chile. Bucca acknowledges support from BIO fellowship Chile-US (Fulbright-CONICYT).

References

- Aron, F., R. W. Allmendinger, J. Cembrano, G. González, and G. Yáñez (2013), Permanent fore-arc extension and seismic segmentation: Insights from the 2010 Maule earthquake, Chile, *J. Geophys. Res. Solid Earth*, 118(2), 724–739, doi:10.1029/2012JB009339.
- Aron, F., J. Cembrano, F. Astudillo, R. W. Allmendinger, and G. Arancibia (2015), Constructing forearc architecture over megathrust seismic cycles: geological snapshots from the Maule earthquake region, Chile, *Geol. Soc. Am. Bull.* 127 (3–4), 464–479, doi: 10.1130/B31125.1.
- Baker, A., R. W. Allmendinger, L. A. Owen, and J. A. Rech (2013), Permanent deformation caused by subduction earthquakes in northern Chile, *Nat. Geosci.*, advance online publication, doi:10.1038/ngeo1789.
- Dielförder, A., H. Vollstaedt, T. Vennemann, A. Berger, and M. Herwegh (2015), Linking megathrust earthquakes to brittle deformation in a fossil accretionary complex, *Nat. Commun.*, 6, doi:10.1038/ncomms8504.
- Ekström, G., M. Nettles, and A. M. Dziewoński (2012), The global CMT project 2004–2010: Centroid-moment tensors for 13,017 earthquakes, *Phys. Earth Planet. Inter.*, 200–201, 1–9, doi:10.1016/j.pepi.2012.04.002.
- Frohlich, C. (1992), Triangle diagrams: ternary graphs to display similarity and diversity of earthquake focal mechanisms, *Phys. Earth Planet. Inter.*, 75(1–3), 193–198, doi:10.1016/0031-9201(92)90130-N.
- Gomberg, J., and B. Sherrod (2014), Crustal earthquake triggering by modern great earthquakes on subduction zone thrusts, *J. Geophys. Res. Solid Earth*, 119(2), 2012JB009826, doi:10.1002/2012JB009826.
- Hardebeck, J. L. (2012), Coseismic and postseismic stress rotations due to great subduction zone earthquakes, *Geophys. Res. Lett.*, 39(21), n/a–n/a, doi:10.1029/2012GL053438.
- Hasegawa, A., K. Yoshida, Y. Asano, T. Okada, T. Iinuma, and Y. Ito (2012), Change in stress field after the 2011 great Tohoku-Oki earthquake, *Earth Planet. Sci. Lett.*, 355–356, 231–243, doi:10.1016/j.epsl.2012.08.042.
- Hayes, G. P., D. J. Wald, and R. L. Johnson (2012), Slab1.0: A three-dimensional model of global subduction zone geometries, *J. Geophys. Res. Solid Earth*, 117(B1), B01302–, doi:10.1029/2011JB008524.
- Lange, D. et al. (2012), Aftershock seismicity of the 27 February 2010 Mw 8.8 Maule earthquake rupture zone, *Earth Planet. Sci. Lett.*, 317–318, 413–425, doi:10.1016/j.epsl.2011.11.034.
- Li, S., M. Moreno, M. Rosenau, D. Melnick, and O. Oncken (2014), Splay fault triggering by great subduction earthquakes inferred from finite element models, *Geophys. Res. Lett.*, 41(2), 2013GL058598, doi:10.1002/2013GL058598.
- Plafker, G. (1967), Surface faults on Montague Island associated

with the 1964 Alaska earthquake, US Geol. Surv. Prof. Pap., 543-G, 42 p.

Sibuet, J.-C. et al. (2007), 26th December 2004 great Sumatra–Andaman earthquake: Co-seismic and post-seismic motions in northern Sumatra, *Earth Planet. Sci. Lett.*, 263(1–2), 88–103.